Journal of the European Ceramic Society 21 (2001) 1569–1572
www.elsevier.com/locate/jeurceramsoc

Synthesis and dielectric properties of $Sr_xBa_{1-x}Nb_2O_6$ formed by YAG laser ablation

K. Kakimoto *, H. Kakemoto, A. Baba, S. Fujita, Y. Masuda

JSPS Research Project, Hachinohe Institute of Technology, 88-1 Oobiraki, Myo, Hachinohe, Aomori 031-8501, Japan

Received 4 September 2000; received in revised form 23 October 2000; accepted 15 November 2000

Abstract

Tungsten-bronze type tetragonal $Sr_xBa_{1-x}Nb_2O_6$ (SBN) ceramics have been synthesized by pressure-less sintering at 1250°C through a mixed-oxide route. With increasing x value in the range from 0.3 to 0.6, the Curie temperature shifted to lower temperature, but the corresponding maximum dielectric constant increased. Further, $Sr_{0.3}Ba_{0.7}Nb_2O_6$ thin films have been formed by pulsed YAG laser deposition (PLD) technique using a selected SBN bulk target with various choices of the deposition parameters. When Pt-coated Si substrates were used for PLD, a preferential c-axis-ordered structure was observed in the films deposited using an energy density above 2.0 J/cm^2, at a substrate temperature above 650°C, and in oxygen partial pressure below 7 Pa. The thin film yielded a rhomboidal P–E hysteresis loop, and showing a remanent polarization (P_r) of 3.1 μ C/cm^2 and coercive field (E_c) of 1.28 kV/cm.

Keywords: Ferroelectric properties; Films; Niobates

1. Introduction

Ferroelectric $Sr_xBa_{1-x}Nb_2O_6$ (SBN) shows tetragonal tungsten bronze structure and is well known to exhibit an extremely high electro-optic coefficient[1] and strong photorefractive effects.[2] Various fabrication techniques have been applied for successful synthesis of SBN in the forms of single crystals,[3] bulk ceramics[4,5] and thin films.[6–11] Especially, the number of reports on the preparation of SBN thin films by pulsed laser deposition (PLD) has remarkably increased in recent years.[9–11] One of the most important advantages of employing PLD to synthesize oxide thin films is the fact that the composition is easily transferred from the sintered bulk target to the deposited film, since the film deposition can be carried out under an ambient of the desired pressure, even for oxidative atmosphere.

In this study, SBN bulk ceramics with various x values were fabricated through a conventional mixed-oxide route, then the PLD technique using YAG laser beam ($\lambda = 266$ nm) was applied for the preparation of SBN thin films from a selected bulk target. Their microstructure and dielectric properties were investigated.

2. Experimental procedure

The raw materials used in this experiment were high-purity powders of $SrCO_3$ (Kanto Chemical Co., 99.6%), $BaCO_3$ (Shin Nippon Chemical Co., 99.97%) and Nb_2O_5 (Kanto Chemical Co., 99.95%). All compositions were prepared in accordance with the formula $xSrCO_3 + (1{-}x)\,BaCO_3 + Nb_2O_5 = Sr_xBa_{1-x}Nb_2O_6 + CO_2$, where $x = 0$ to 1.0 at each 0.1 step. The mixed powders were ball-milled for 24 h in methanol. The dried material was crushed and sieved, followed by uni-axial pressing at 100 MPa into cylindrical forms (ϕ: 20 mm, h: 5 mm). The green tablets were calcined at 1000°C for 10 h, then sintered at 1250°C for 10 h. Crystal phase was identified by X-ray diffraction (XRD) using CuK_α radiation. Density was determined from the weight and dimensions, and compared with the density calculated from the lattice parameters that were determined by XRD data.

* Corresponding author. Tel.: +81-178-25-8162; fax: +81-178-25-1430.

E-mail address: kakimoto@hi-tech.ac.jp (K. Kakimoto).

0955-2219/01/$ - see front matter
PII: S0955-2219(01)00066-8

SBN thin films were deposited using PLD technique. A YAG laser beam (Spectron Laser System SL850) with a wavelength $\lambda = 266$ nm (the forth harmonic generation, FHG) and a repetition rate of 10 Hz was focused onto a rotating, sintered $Sr_{0.3}Ba_{0.7}Nb_2O_6$ target. The fluence of the incident laser beam was varied from 0.9 to 3.2 J/cm^2 and the base pressure of the vacuum chamber was in the 10^{-5} Pa range. Films were deposited on quartz or Pt-coated Si substrates heated in the temperature range between 500 and 700°C, under oxygen partial pressure ambient of 1–9 Pa, followed by rapid thermal annealing (RTA) at 800°C under an oxygen atmosphere. The films were analyzed by XRD, X-ray fluorescence spectroscopy (XRF) and atomic force microscopy (AFM). For electrical measurements, Au top electrode was sputtered on the film. Dielectric properties were measured at room temperature in the frequency range of 1–1000 kHz using an LCR meter (HP 4284A). Temperature dependence of permittivity ε at 1 kHz was investigated at elevated temperature up to 350°C. *D–E* hysteresis loops were observed using a Sawyer-Tower circuit.

3. Results and discussion

3.1. SBN bulk target

SBN bulk specimens showed relatively good sintering behaviors without coarse grains and large pores. XRD measurement indicated those SBN bulk specimens with x of 0.3–0.7 showed a single tetragonal phase [see Fig. 1(a)], while the specimens with higher Sr contents over $x=0.7$ additionally contained small amounts of orthorhombic strontium niobate phases. The lattice parameter of *a*-, *c*-axis, and the corresponding c/a ratio for the tetragonal specimens gradually decreased with increasing x value, and the specimens exhibited 84–95% theoretical densities. Fig. 2 shows the temperature dependence of ε at 1 kHz for several SBN bulk specimens. The Curie temperature (T_c) which corresponds to the peak position of ε shifts to lower temperatures with increasing x value, which may be caused by different local configurations in the tetragonal tungsten bronze (TTB) structure.[12] T_c varies widely from 275°C for $x=0.2$ to 58°C for $x=0.6$. Similar T_c variation depending SBN composition has been reported both for single crystals[13] and polycrystals.[5] In addition to the configuration effect, VanDamme et al.[5] discussed such a T_c variation from a viewpoint of microstructure difference, i.e. grain size and its uniformity for the polycrystalline SBN specimens. They compared several specimens prepared by pressure-less sintering at different temperatures and post-HIP treatment. The specimens showed different TTB crystallinities and grain sizes, which resulted in a T_c variation in spite of the same SBN composition. Therefore, synergic effects due to configuration and microstructure differences seem to appear in the temperature dependence of ε for polycrystalline SBN bulk ceramics. On the other hand, the maximum values of ε shown in Fig. 2 increase with increasing x value, but are much smaller than those for single crystals because of less preferential orientation in crystallinity. Dielectric loss tangent (tan δ) at the Curie temperature kept 0.03 or less for SBN specimens with x of 0.2–0.6. In particular, tan δ of the specimens with x of 0.2 and 0.3 remained 0.02 up to 300°C and exhibited only a slight increase from 0.02 at 1 kHz to 0.04 at 1000 kHz in room-temperature measurement. The other specimens showed much larger tan δ in the measurements at elevated temperature and at various frequency levels from 1 to 1000 kHz.

The remanent polarization (P_r) and coercive field (E_c) were estimated from the electrical polarization — electrical field (*P–E*) hysteresis loops recorded at room temperature. Fig. 3 summarizes those values for the SBN specimens with x of 0–1.0. The SBN specimens with x of 0, 0.8, 0.9 and 1.0 showed linear P–E relationships, and no P_r and E_c were observed. In contrast, the SBN specimens with x of 0.2–0.7 demonstrated ferroelectric *P–E* hysteresis loops, but an ellipsoidal shape was observed for $x=0.2$ while typical rhomboidal

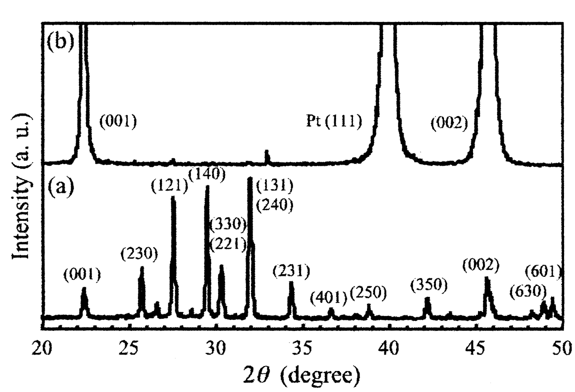

Fig. 1. XRD patterns of (a) sintered $Sr_{0.3}Ba_{0.7}Nb_2O_6$ bulk specimen and (b) thin film prepared by PLD on Pt/Si substrate.

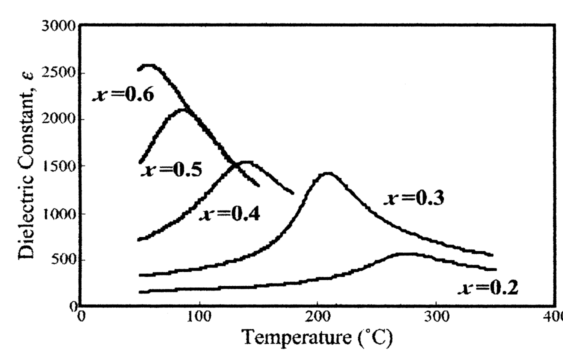

Fig. 2. Temperature dependence of dielectric constant ε at 1 kHz for $Sr_xBa_{1-x}Nb_2O_6$ bulk specimens with x of 0.2–0.6.

shapes appeared for the other specimens. P_r shows a maximum value of 1.65 μC/cm^2 at $x=0.5$, and E_c decreases with increasing x value from 0.2 to 0.7.

It is evident from the above results that the SBN bulk specimen with x of 0.3 has superior ferroelectric properties to the others in that it shows a relatively high T_c of 208°C, low tan δ at elevated temperature and at wide range of frequency, and demonstrated a rhomboidal *P–E* hysteresis loop. Therefore, the SBN bulk specimen with x of 0.3 was selected as a target source for synthesizing $Sr_{0.3}Ba_{0.7}Nb_2O_6$ thin films by the PLD method.

3.2. SBN thin film

Prior to deposition on Si-based substrate, quartz substrate was used for investigating the dependence of PLD conditions on characteristics of $Sr_{0.3}Ba_{0.7}Nb_2O_6$ thin films. When PLD was employed under an oxygen partial pressure (P_{O_2}) of 5 Pa at a substrate temperature (T_{sub}) of 700°C, increasing fluence of the incident laser beam onto the target from 0.9 to 3.2 J/cm^2 enhanced a film deposition rate from 5.8 to 23.5 nm/min. A single TTB phase also became dominant above 2.1 J/cm^2. The TTB phase started to appear at higher T_{sub} above 650°C. The deposited SBN thin film showed almost the same cation composition as the bulk target, and the composition was little affected by applied P_{O_2} ranging from 1 to 9 Pa. However, the formed grain size dramatically decreased with increasing applied P_{O_2}. The average sizes are estimated to be around 200 nm for 1 Pa and 50 nm for 7 Pa, as shown in Fig. 4. The reason seems to be that increasing P_{O_2} reduced the grain mobility to form accumulated large grains. No obvious grain shape was observed for P_{O_2} of 9 Pa in this experiment. Therefore, lower P_{O_2} is advantageous for preparing $Sr_{0.3}Ba_{0.7}Nb_2O_6$ thin films with relatively large grains that has a potential for exhibiting large P_r values. However, a slight color change from half-transparency into dark brown was observed for the thin films fabricated by lowering P_{O_2}. This seems to be caused by oxygen deficiency from its stoichiometric composition, thereby requiring post-annealing treatment under an oxygen ambient in order to reduce a leakage current density.

A similar PLD condition dependence, i.e. laser fluence, P_{O_2} and T_{sub} on the film characteristics was observed also in the $Sr_{0.3}Ba_{0.7}Nb_2O_6$ thin films deposited on Pt-coated Si substrates. An average grain size of the film at P_{O_2} of 1 Pa was estimated to be around 300 nm that was 1.5 times larger than the film deposited on quartz substrate. Moreover, the film demonstrated a highly preferential *c*-axis orientation [Fig. 1(b)] after the O_2 annealing treatment. Highly textured *c*-axis orientation is required to optimize the ferroelectric properties of the films, since the c-axis is the orientation of spontaneous polarization. Fig. 5 compares the temperature dependence of ε at 1 kHz for the $Sr_{0.3}Ba_{0.7}Nb_2O_6$ thin film with that for the bulk target used. It is obvious that a highly preferential *c*-axis orientation allows high ε for the thin film at all temperatures investigated. The film shows a maximum ε of 3500 that is much larger than 1500 for the bulk target showing a polycrystalline orientation. Further, it is interesting to note that the Curie temperature increases from 208°C for the bulk target to 230°C for the film. This difference seems to be explained on the basis of microstructural differences between the bulk target and thin film, which is mentioned in the previous section, but at present, we are unable to give any qualitative explanation for the present experimental result. Fig. 6 shows a rhomboidal *P–E*

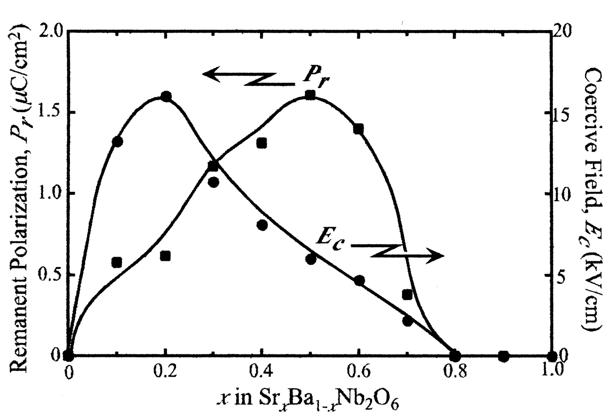

Fig. 3. Remanent polarization P_r and coercive field E_c observed in the *P–E* hysteresis loops recorded at room temperature for $Sr_xBa_{1-x}Nb_2O_6$ bulk specimens with x of 0–1.0.

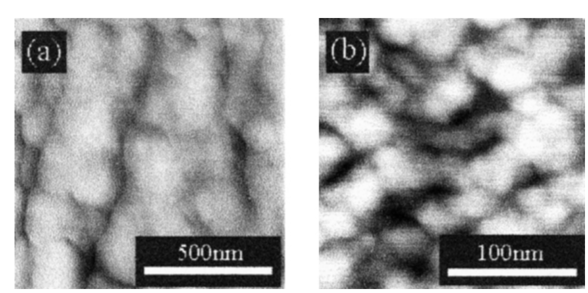

Fig. 4. AFM images of $Sr_{0.3}Ba_{0.7}Nb_2O_6$ thin films under different oxygen partial pressure of (a) 1 Pa and (b) 7 Pa during PLD proces-

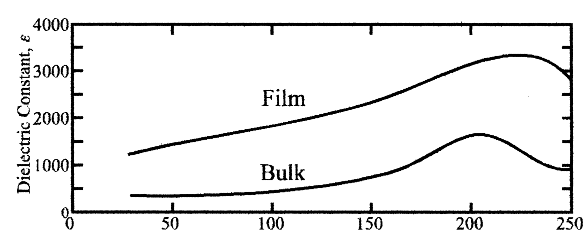

Fig. 5. Comparison of temperature dependence of dielectric constant ε at 1 kHz for the $Sr_{0.3}Ba_{0.7}Nb_2O_6$ thin film with that for the bulk target shown in Fig. 2.

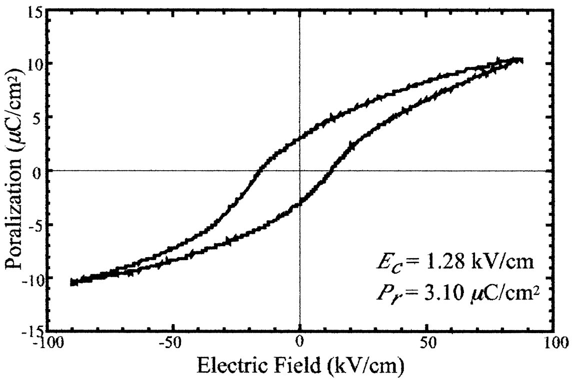

Fig. 6. *P–E* hysteresis loops recorded at room temperature for the $Sr_{0.3}Ba_{0.7}Nb_2O_6$ thin film.

hysteresis loop for the c-axis oriented thin film. The P_r and E_c of this film were measured to be 3.1 $\mu C/cm^2$ and 1.28 kV/cm, respectively. Much higher P_r was obtained for the *c*-axis oriented thin film than that for its bulk target shown in Fig. 3 ($x=0.3$).

4. Conclusion

The SBN bulk ceramics demonstrated attractive behaviors in that the Curie temperature shifted to lower temperature, but the corresponding maximum dielectric constant increased with increasing *x* value in the range from 0.3 to 0.6. This seems to meet a wide range of commercial requests for many applications by selection of the desired SBN composition. In order for the ferroelectric SBN thin film to meet these requests, a superior stoichiometric control as well as texture control for an excellent spontaneous polarization is required. YAG laser has superior advantages especially in running cost, easy maintenance and safety to excimer lasers. Pulsed FHG–YAG laser deposition (PLD) was proved for the thin film to demonstrate an excellent composition agreement with its bulk target. The PLD-derived $Sr_{0.3}Ba_{0.7}Nb_2O_6$ thin film on Pt-coated Si substrate demonstrated a preferential *c*-axis-oriented structure, thereby showing a relatively good ferroelectric *P–E* hysteresis loop.

Acknowledgements

This work was financially supported by the Next Generation of Research for the Future, Japan Society for the Promotion of Science (JSPS-RFTF 96P00105) and a commission research grant given to Y.M. from Tokin Co. Ltd., Japan.

References

1. Lenzo, P. V., Spencer, E. G. and Ballman, A. A., Electro-optic coefficients of ferroelectric strontium barium niobate. *Appl. Phys. Lett.*, 1967, **11**, 23–24.
2. Neurgaonkar, R. R. and Cory, W. K., Progress in photorefractive tungsten bronze crystals. *J. Opt. Soc. Am. B: Opt. Phys.*, 1986, **3**, 274–282.
3. Ballman, A. A. and Brown, H., The growth and properties of strontium barium metaniobate, $Sr_xBa_{1-x}Nb_2O_6$, a tungsten bronze ferroelectric. *J. Cryst. Growth*, 1967, **1**, 311–314.
4. Nagata, K., Yamamoto, Y., Igarashi, H. and Okazaki, K., Properties of the hot-pressed strontium barium niobate ceramics. *Ferroelectrics*, 1981, **38**, 853–856.
5. VanDamme, N. S., Sutherland, A. E., Jones, L., Bridger, K. and Winzer, S. R., Fabrication of optically transparent and electro-optic strontium barium niobate ceramics. *J. Am. Ceram. Soc.*, 1991, **74**, 1785–1792.
6. Neurgaonker, R. R. and Wu, E. T., Epitaxial growth of ferroelectric T. B. $Sr_xBa_{1-x}Nb_2O_6$ films for optoelectronic applications. *Mater. Res. Bull.*, 1987, **22**, 1095–1102.
7. Chen, C. J., Xu, Y, Xu, R. and Mackenzie, J. D., Ferroelectric $Sr_{1-x}Ba_xNb_2O_6$ (SBN) thin film derived by sol-gel technique. *Ceram. Trans.*, 1990, **14**, 211–218.
8. Yang, Y. S., Ryu, M. K., Joo, H. J., Lee, S. H., Lee, S. J., Kang, K. Y. and Jang, M. S., Ferroelectricity and electronic defect characteristics of c-oriented $Sr_{0.25}Ba_{0.75}Nb_2O_6$ thin films deposited on si substrates. *Appl. Phys. Lett.*, 2000, **76**, 3472–3474.
9. Schwyn Thöny, S., Youden, K. E., Harris, J. S. Jr. and Hasselink, L., Growth of epitaxial strontium barium niobate thin films by pulsed laser deposition. *Appl. Phys. Lett.*, 1994, **65**, 2018–2020.
10. Lin, W., Tseng, T., Lin, S., Tu, S., Yang, S., Harn, J., Liu, K. and Lin, I., Growth of epitaxial-like $(Sr_{0.5}Ba_{0.5})Nb_2O_6$ ferroelectric films. *Jpn. J. Appl. Phys.*, 1995, **34**, L625–L627.
11. Cheng, H., Hu, C. and Lin, I., Influence of Pt, RuO_2 and $SrRuO_3$ intermediate layers on characteristics of $(Sr_{0.5}Ba_{0.5})$ Nb_2O_6 thin films. *Jpn. J. Appl. Phys.*, 1997, **36**, 284–288.
12. Ngai, K. L. and Reinecke, T. L., Model of the ferroelectric phase transition in the tetragonal tungsten-bronze-structure ferroelectrics. *Phys. Rev. Lett.*, 1977, **38**, 74–77.
13. Glass, A. M., Investigation of the electrical properties of $Sr_{1-x}Ba_xNb_2O_6$ with special reference to pyroelectric detection. *J. Appl. Phys.*, 1969, **40**, 4699–4713.